Polynuclear Homo- or Heterometallic Palladium(II)−Platinum(II) Pentafluorophenyl Complexes Containing Bridging Diphenylphosphido Ligands. 6.† Syntheses and Molecular Structure of $[Pt_4(\mu_2\text{-}PPh_2)_4(C_6F_5)_4(CO)_2]\cdot 2CH_2Cl_2$ and $[Pt_2Pd_2(\mu_2\text{-}PPh_2)_2(\mu_3\text{-}PPh(1,2\text{-}\eta^2\text{-}Ph)\text{-}\kappa^3P)(C_6F_5)_3(CO)(PPh_2C_6F_5)]\cdot CHCl_3\cdot C_5H_{12}$‡

Larry R. Falvello, Juan Forniés,* Consuelo Fortuño, Antonio Martín, and Ana P. Martínez-Sariñena

Departamento de Química Inorgánica and Instituto de Ciencia de Materiales de Aragón, Universidad de Zaragoza-CSIC, 50009 Zaragoza, Spain

Received July 28, 1997⊗

The reaction of $[NBu_4]_2[\{(C_6F_5)_2Pt(\mu\text{-}PPh_2)_2Pt(\mu\text{-}Cl)\}_2]$, **A**, with CO in CH_2Cl_2 gives the expected dinuclear compound $[NBu_4][(C_6F_5)_2Pt(\mu\text{-}PPh_2)_2PtCl(CO)]$, **1**, which reacts with $AgClO_4$ (1:1 molar ratio) in CH_2Cl_2 to produce the tetranuclear cluster $[Pt_4(\mu\text{-}PPh_2)_4(C_6F_5)_4(CO)_2]$, **2**. The analogous complex $[NBu_4]_2[\{(C_6F_5)_2Pt(\mu\text{-}PPh_2)_2Pd(\mu\text{-}Cl)\}_2]$, **B**, does not react with CO under similar conditions, but treatment of **B** with $AgClO_4$ (1:2 molar ratio, CH_2Cl_2) renders the tetranuclear compound $[Pt_2Pd_2(\mu\text{-}PPh_2)_3(C_6F_5)_3(PPh_2C_6F_5)]$, **3**, in which the $PPh_2C_6F_5$ ligand is produced through an unusual $M-PPh_2/M-C_6F_5$ reductive coupling. Complex **3** reacts with CO in CH_2Cl_2 producing the tetranuclear complex $[Pt_2Pd_2(\mu\text{-}PPh_2)_2(\mu_3\text{-}PPh(1,2\text{-}\eta^2\text{-}Ph)\text{-}\kappa^3P)(C_6F_5)_3(CO)(PPh_2C_6F_5)]$, **4**. The molecular structures of complexes **2** and **4** have been established by X-ray crystallography.

Introduction

It is well-known that phosphido groups are very flexible ligands which are able to stabilize polynuclear transition metal clusters.[1] In the course of our current research on phosphido palladium or platinum complexes, we have synthesised the tetranuclear homo- or heterometallic derivatives $[NBu_4]_2[\{(C_6F_5)_2Pt(\mu\text{-}PPh_2)_2M(\mu\text{-}Cl)\}_2]$ (M = Pd, Pt),[2] which react easily with neutral monodentate ligands such as phosphines, giving the dinuclear derivatives as a result of halide bridge cleavage. The ^{31}P NMR spectra of the resulting dinuclear derivatives reveal that the Pt−P−M angle is rather large, i.e., that there is no intermetallic bonding, to be expected for a system with a total valence electron count of 32. In addition, we have also observed that these chloride-containing complexes eliminate chloride, after adequate treatment, forming the dinuclear complexes with Pt→M bonds (total valence electron count 30).

However, preliminary studies on the reactions of the above-mentioned tetranuclear species with CO revealed that the reactions apparently proceeded in a different way that had not been elucidated.

In this paper, we report the reactions of the tetranuclear complexes with CO and describe several polynuclear platinum or palladium carbonyl phosphido complexes which are the result of these or derived reactions and which display several interesting features. Most of them contain several Pt−M bonds and η^2-P(C_6H_5)-(C_6H_5)−M interactions. In one of the reactions, a reductive coupling between PPh_2 and C_6F_5 to produce $PPh_2C_6F_5$, which is an unusual process, is observed.

Results and Discussion

Reaction of $[NBu_4]_2[\{(C_6F_5)_2Pt(\mu\text{-}PPh_2)_2Pt(\mu\text{-}Cl)\}_2]$ with CO. $[NBu_4]_2[\{(C_6F_5)_2Pt(\mu\text{-}PPh_2)_2Pt(\mu\text{-}Cl)\}_2]$ reacts with CO in CH_2Cl_2 producing $Pt(\mu\text{-}Cl)_2Pt$ bridge cleavage and yielding the dinuclear anionic derivative $[NBu_4][(C_6F_5)_2Pt(\mu\text{-}PPh_2)_2PtCl(CO)]$, **1** (see Scheme 1a). The spectroscopic data allow an unequivocal structural assignment for complex **1**. The IR spectrum shows characteristic absorptions of the pentafluorophenyl groups. The ones due to the X-sensitive mode appear as two bands (783, 776 cm^{-1}) with similar intensities, as expected for complexes containing two C_6F_5 groups bonded to the same metal center and in mutually *cis* positions.[3] Absorptions due to ν(Pt−Cl), 270 cm^{-1}, and ν(C≡O), 2075 cm^{-1}, are also observed. The ^{31}P NMR spectrum of **1** can be interpreted in terms of a second-order spin system (AB). The resonances appear upfield, suggesting that no platinum−platinum bond is present,[4] and show platinum satellites. In the ^{19}F NMR spec-

§ Part 5. See ref 7c.

‡ Dedicated to Prof. Pascual Royo on the occasion of his 60th birthday.

⊗ Abstract published in *Advance ACS Abstracts,* December 1, 1997.

(1) Baker, R. T.; Fultz, W. C.; Marder, T. B.; Williams, I. D. *Organometallics* **1990**, *9*, 2357 and references given therein.

(2) (a) Forniés, J.; Fortuño, C.; Navarro, R.; Martínez, F.; Welch, A. J. *J. Organomet. Chem.* **1990**, *394*, 643. (b) Falvello, L. R.; Forniés, J.; Fortuño, C.; Martínez, F. *Inorg. Chem.* **1994**, *33*, 6242.

(3) Usón, R.; Forniés, J. *Adv. Organomet. Chem.* **1988**, *288*, 219.

(4) (a) Mercer, W. C.; Geoffroy, G. L.; Rheingold, A. L. *Organometallics* **1985**, *4*, 1418. (b) Morrison, E. D.; Harley, A. D.; Marcelli, M. A.; Geoffroy, G. L.; Rheingold, A. L.; Fultz, W. C. *Organometallics* **1984**, *3*, 1407. (c) Mercer, W. C.; Whittle, R. R.; Burkhardt, E. W.; Geoffroy, G. L. *Organometallics* **1985**, *4*, 68.

S0276-7333(97)00646-8 CCC: $14.00

Scheme 1

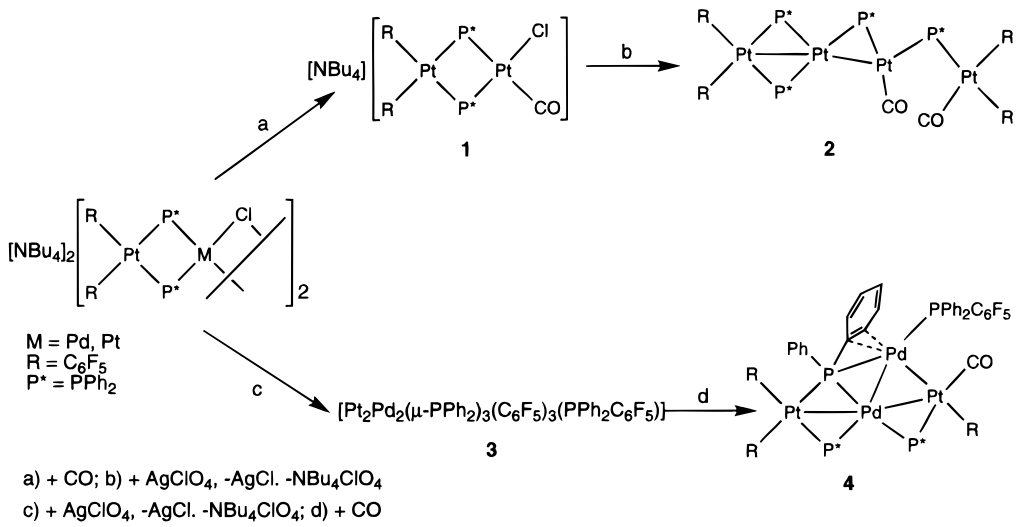

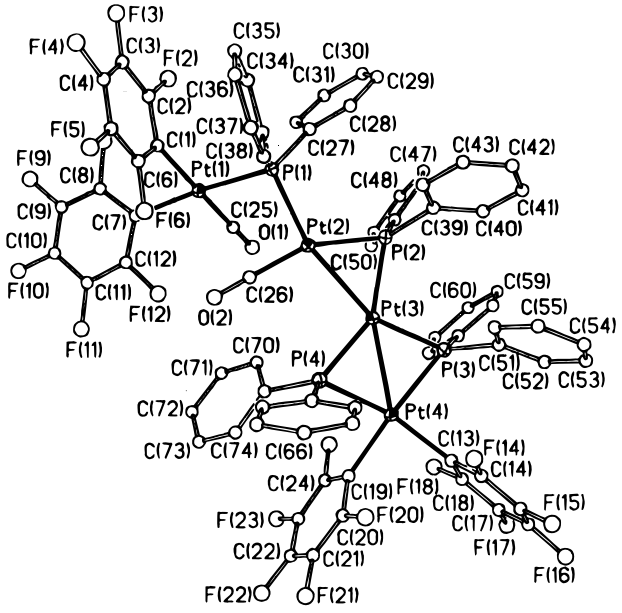

Figure 1. Structure of $[Pt_4(\mu\text{-}PPh_2)_4(C_6F_5)_4(CO)_2]$ (**2**) showing the atom labeling scheme.

trum, the signals due to the *p*-F atoms appear to overlap with the ones due to the *m*-F atoms and signals due to the *o*-F atoms appear as a broad multiplet with platinum satellites.

The reaction of complex **1** with $AgClO_4$ (1:1 molar ratio) in CH_2Cl_2 results in the precipitation of AgCl, and from the mother liquor after appropriate treatment, a compound, **2**, of stoichiometry $[Pt_2(\mu\text{-}PPh_2)_2(C_6F_5)_2(CO)]$ is obtained. However, although this compound has the same stoichiometry as the complexes obtained by reacting the analogous phosphine complexes, the structural data reveal a different structure. Complex **2** can also be obtained by reacting $[NBu_4]_2[\{(C_6F_5)_2Pt(\mu\text{-}PPh_2)_2Pt(\mu\text{-}Cl)\}_2]$ with 2 equiv of $AgClO_4$ and CO. The structure of **2** has been established by an X-ray diffraction study.

Crystal Structure of $[Pt_4(\mu\text{-}PPh_2)_4(C_6F_5)_4(CO)_2]\cdot 2CH_2Cl_2$ ($2\cdot 2CH_2Cl_2$). The structure of complex **2** together with the atom labeling scheme is shown in Figure 1. Selected bond distances and angles are listed in Table 1. Complex **2** is a tetrametallic unit in which the four platinum atoms are bridged by phosphide ligands. The Pt(1)−C and Pt(1)−P(1) distances are in the range usually found for this kind of complex.[2,5] The angles C−Pt(1)−C and C−Pt(1)−P(1) define an almost perfect square-planar environment for the metal atom. The Pt(1) fragment is linked to the rest of the molecule through the P(1)Ph_2 ligand. Pt(2), Pt(3), and Pt(4) and their environments lie in a plane, except for the P(1) atom which is located 0.665 Å above the plane. This plane makes a dihedral angle of 53.0° with the square coordination plane of Pt(1). The angle Pt(1)−P(1)−Pt(2) is 102.14(9)°, and the Pt(1)−Pt(2) distance is 3.632(1) Å, excluding any kind of interaction between the metal centers.

Table 1. Selected Bond Lengths (Å) and Angles (deg) for $[Pt_4(C_6F_5)_4(PPh_2)_4(CO)_2]$ ($2\cdot 2CH_2Cl_2$)

Pt(1)−C(25)	1.917(10)	Pt(2)−Pt(3)	2.6994(5)
Pt(1)−P(1)	2.354(2)	Pt(3)−P(2)	2.264(2)
Pt(2)−P(1)	2.315(2)	Pt(4)−C(13)	2.080(9)
Pt(3)−P(4)	2.247(2)	Pt(1)−C(7)	2.073(9)
Pt(4)−C(19)	2.056(9)	Pt(2)−P(2)	2.247(2)
Pt(4)−P(4)	2.330(2)	Pt(3)−P(3)	2.237(2)
Pt(1)−C(1)	2.040(8)	Pt(3)−Pt(4)	2.6882(5)
Pt(2)−C(26)	1.917(10)	Pt(4)−P(3)	2.288(2)
C(25)−Pt(1)−C(1)	177.0(4)	C(25)−Pt(1)−C(7)	89.5(4)
C(1)−Pt(1)−C(7)	89.1(4)	C(25)−Pt(1)−P(1)	91.7(3)
C(1)−Pt(1)−P(1)	90.1(3)	C(7)−Pt(1)−P(1)	172.2(3)
C(26)−Pt(2)−P(2)	157.9(3)	C(26)−Pt(2)−P(1)	96.6(3)
P(2)−Pt(2)−P(1)	105.56(8)	C(26)−Pt(2)−Pt(3)	104.6(3)
P(2)−Pt(2)−Pt(3)	53.53(6)	P(1)−Pt(2)−Pt(3)	156.89(6)
P(3)−Pt(3)−P(4)	109.73(8)	P(3)−Pt(3)−P(2)	102.85(8)
P(4)−Pt(3)−P(2)	147.35(8)	Pt(2)−P(1)−Pt(1)	102.14(9)
Pt(2)−P(2)−Pt(3)	73.52(7)	Pt(3)−P(3)−Pt(4)	72.90(7)
Pt(3)−P(4)−Pt(4)	71.91(7)		

Pt(2) and Pt(3) are bridged by a single phosphido ligand. The small value of the Pt(2)−P(2)−Pt(3) angle (73.52(7)°) and the short Pt(2)−Pt(3) distance (2.6994(5) Å) are consistent with the presence of an intermetallic bond. The Pt(2) and Pt(3) environments are distorted from square planar (Table 1).

Pt(3) and Pt(4) are bridged by two phosphido ligands, the Pt(3)−Pt(4) distance being 2.6882(5) Å. The values of the angles Pt(3)−P−Pt(4) (72.90(7)° for P(3) and 71.91(7)° for P(4)]) are small, and the P(3)−Pt−P(4) angles (109.73(8)° for Pt(3) and 105.13(8)° for Pt(4)) are

(5) (a) Alonso, E.; Forniés, J.; Fortuño, C.; Martín, A.; Orpen, A. G. *J. Chem. Soc., Chem. Commun.* **1996**, 231. (b) Alonso, E.; Forniés, J.; Fortuño, C.; Tomás, M. *J. Chem. Soc., Dalton Trans.* **1995**, 3777.

relatively large. This kind of geometry is commonly found for fragments $M(\mu\text{-}PPh_2)_2M'$ in which metal−metal bonds are invoked[6] and are rather similar to that found in the complex $[(C_6F_5)_2Pt(\mu\text{-}PPh_2)_2Pd(PPh_3)]$.[2b] Pt(4) is also bonded to two pentafluophenyl ligands, thus completing the square-planar coordination sphere.

It is noteworthy that the structure of **2** shows phosphido ligands acting as bridges in three structurally different forms. Phosphide P(1) is the only ligand bridging the two platinum atoms, Pt(1) and Pt(2), with no intermetallic interaction. Phosphide P(2) is the only ligand linking Pt(2) and Pt(3), but in this case the Pt−Pt distance is consistent with a Pt−Pt bond. Finally Pt(3) and Pt(4) are bridged simultaneously by two phosphide ligands, with a short intermetallic distance as well. This structure gives a total valence electron count of 60, which is consistent with the presence of two Pt−Pt bonds between three Pt(II) centers in the bent-chain cluster **2**.

The IR spectrum of **2** shows no absorptions assignable to ν(Pt−Cl). The X-sensitive modes of the C_6F_5 groups appear as two broad absorptions of different intensities. Moreover, complex **2** shows two sharp absorptions at 2082 and 2056 cm^{-1} due to the ν(C≡O) stretching modes. All of these data are in accord with the structure of **2**.

It is well-documented that a deshielding of the ^{31}P resonances in phosphido-bridged complexes may indicate the presence of a metal−metal bond.[4] The ^{31}P NMR spectrum of **2** in $CDCl_3$ shows four signals at higher frequencies than the corresponding signals from the starting material. Signals due to P(4) and P(3) (P atoms of PPh_2 groups that bridge two platinum centers joined by a metal−metal bond) appear at 275.7 and 257.2 ppm, respectively. Analogous chemical shifts have been found for other complexes that show the fragment "$(C_6F_5)_2Pt(\mu\text{-}PPh_2)_2M$" with short Pt−M distances.[2b] The $P(2)Ph_2$ group acts as a single bridging ligand between the Pt(3) and Pt(2) centers (Pt(3)−Pt(2) distance 2.6994(5) Å), and the signal due to P(2) appears at 147.1 ppm, in the same region as that found for the analogous PPh_2 in $[NBu_4][Pt_3(\mu\text{-}PPh_2)_2(C_6F_5)_5]$.[5a] The signal due to P(1) appears at a lower frequency, −6.9 ppm, in good agreement with the long Pt(1)−Pt(2) distance and with the $\delta^{31}P$ found for other singly bridged μ-phosphido dinuclear complexes without metal−metal bonds.[7] A relationship between the angular parameters at the phosphorus atom and the corresponding $\delta^{31}P$ has been previously proposed. Thus, the closing of the M−P−M′ angle means a deshielding at the P atom.[8] In fact, the Pt(1)−P(1)−Pt(2) angle (102.14(9)°) is the largest one in cluster **2**. Nevertheless, if we compare this angle and the $\delta^{31}P$ for this phosphide ligand with the M−P−M angles observed in our doubly bridged bis(diphenylphosphido) previously reported complexes, in which no metal−metal bond is present (102.7° and 103.2°, $\delta^{31}P = -132.0$ ppm for $[(C_6F_5)_2Pt(\mu\text{-}PPh_2)_2Pt(phen)]$;[2a] 104.4° and 102.3°, $\delta^{31}P = -126.8$ ppm for $[(C_6F_5)_2Pt(\mu\text{-}PPh_2)_2Pd(\mu\text{-}OH)_2Pt(PPh_3)_2]$[5b]), we and others[9] conclude that this relationship may not always be true. Thus, $\delta^{31}P$ values can render important information about M−P−M angles in singly bridged diphenylphosphido or in dibridged bis(diphenylphosphido) complexes, but single and double bridges cannot be compared between them for this purpose.

All signals show platinum satellites, and from each of the satellites, two $^1J_{Pt-P}$ values can be extracted. Powell[10] correlated Pt−P_μ bond lengths with $^1J_{Pt-P_\mu}$ values in closely related dinuclear systems, the longer Pt−P bonds being associated with a decrease in the coupling constant. Nevertheless, as he pointed out, $^1J_{Pt-P_\mu}$ values are very sensitive to changes in ligands on the Pt center. In agreement with this, we observed that while the Pt(2)−P(2) distance is equal to Pt(3)−P(4), the two $^1J_{Pt-P(2)}$ values are much larger than that found for $^1J_{Pt(3)-P(4)}$. Hence, an unequivocal assignment of $^1J_{Pt-P(2)}$ and $^1J_{Pt-P(1)}$ values is not possible in this case.

The formation of this tetranuclear compound instead of the expected dinuclear derivative could be a consequence of the interaction between the two moieties of the expected dinuclear derivative, since in such a compound the platinum center of the Pt−CO fragment displays a Lewis acid behavior[2b] while both Pt−P bonds of the same fragment behave as a Lewis base,[11,12] so that a donor−acceptor interaction could start the dimerization process giving the intermediate **A** which could rearrange to **B** and finally to **2** (see Scheme 2).

Reaction of $[NBu_4]_2[\{(C_6F_5)_2Pt(\mu\text{-}PPh_2)_2Pd(\mu\text{-}Cl)\}_2]$ with CO. The analogous reaction between the heteronuclear compound and CO gives completely different results. When a CH_2Cl_2 solution of $[NBu_4]_2[\{(C_6F_5)_2Pt(\mu\text{-}PPh_2)_2Pd(\mu\text{-}Cl)\}_2]$ is treated with CO (at room temperature), in order to obtain $[NBu_4][(C_6F_5)_2Pt(\mu\text{-}PPh_2)_2PdCl(CO)]$, no reaction takes place and only the starting material can be recovered from the mother liquor. The carbon monoxide is not able to break the "$Pd(\mu\text{-}Cl)_2Pd$" framework to give a Pd−CO bond. For that reason, and aiming to prepare a polynuclear palladium/platinum complex containing carbonyl, we have changed the synthetic strategy in order to force the chloride elimination reaction. So, when an orange solution of $[NBu_4]_2[\{(C_6F_5)_2Pt(\mu\text{-}PPh_2)_2Pd(\mu\text{-}Cl)\}_2]$ in CH_2Cl_2 is treated with $AgClO_4$ (molar ratio 1:2), its color changes to dark purple, and from the solution a compound of stoichiometry $[Pt_2Pd_2(\mu\text{-}PPh_2)_3(C_6F_5)_3(PPh_2C_6F_5)]$, **3**, is isolated in high yield (see Scheme 1c). A CH_2Cl_2 solution of complex **3** reacts with CO at room temperature to give the carbonyl cluster $[Pt_2Pd_2(\mu\text{-}PPh_2)_3(C_6F_5)_3(PPh_2C_6F_5)(CO)]$, **4**. The IR and ^{19}F NMR spectra of the two complexes **3** and **4** present some similarities. A full structural characterization of **4** has been carried out by X-ray diffraction, and from these data and by comparing the spectroscopic data of **3** and **4**, a reasonable structure of complex **3** can finally be proposed.

(6) (a) Braunstein, P.; Matt, D.; Bars, O.; Louer, M.; Grandjean, D.; Fischer, J.; Mitschler, A. *J. Organomet. Chem.* **1981**, *213*, 79. (b) Shyu, S.-G.; Calligaris, M.; Nardin, G.; Wojcicki, A. *J. Am. Chem. Soc.* **1987**, *109*, 3617.

(7) (a) Shyu, S.-G.; Lin, P.-J.; Lin, K.-J.; Chang, M.-C.; Wen, Y.-S. *Organometallics* **1995**, *14*, 2253. (b) Shyu, S.-G.; Hsiao, S.-M.; Lin, K.-J.; Gau, H.-M. *Organometallics* **1995**, *14*, 4300. (c) Alonso, E.; Forniés, J.; Fortuño, C.; Martín, A.; Rosair, G. M.; Welch, A. J. *Inorg. Chem.* **1997**, *36*, 4426.

(8) Barré, C.; Boudot, P.; Kubicki, M. M.; Moise, C. *Inorg. Chem.* **1995**, *34*, 284.

(9) Deeming, A. J.; Doherty, S. *Polyhedron* **1996**, *15*, 1175.

(10) (a) Powell, J.; Sawyer, J. F.; Stainer, M. V. R. *Inorg. Chem.* **1989**, *28*, 4461. (b) Powell, J.; Fuchs, E.; Gregg, M. R.; Phillips, J.; Stainer, M. V. R. *Organometallics* **1990**, *426*, 247.

(11) Alonso, E. Ph.D. Thesis, University of Zaragoza, Zaragoza, Spain, July 1996.

(12) Bender, R.; Braunstein, P.; Dedieu, A.; Dusausoy, Y. *Angew. Chem., Int. Ed. Engl.* **1989**, *28*, 923.

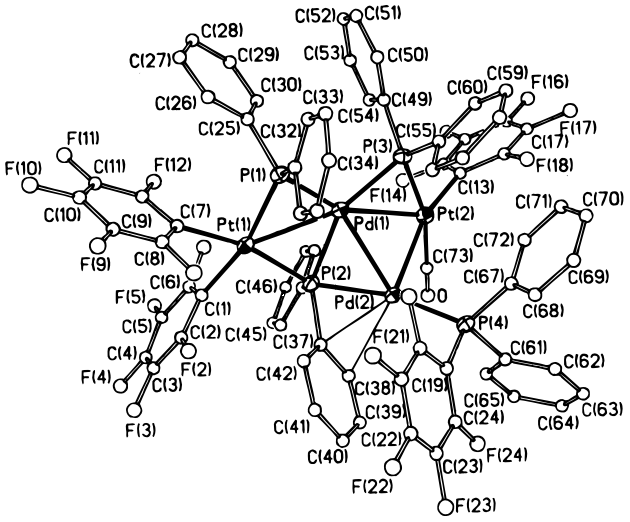

Figure 2. Structure of $[Pt_2Pd_2(\mu\text{-}PPh_2)_3(C_6F_5)_3(PPh_2C_6F_5)\text{-}(CO)]$ (**4**) showing the atom labeling scheme.

Scheme 2

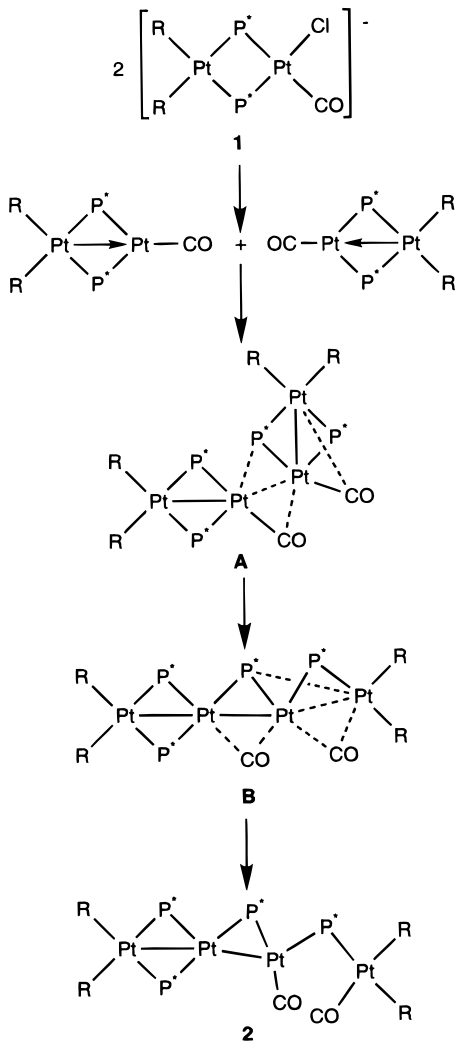

Crystal Structure of $[Pt_2Pd_2(\mu\text{-}PPh_2)_3(C_6F_5)_3\text{-}(PPh_2C_6F_5)(CO)]\cdot CHCl_3\cdot C_5H_{12}$ ($4\cdot CHCl_3\cdot C_5H_{12}$). The structure of complex **4** together with the atom labeling scheme is shown in Figures 2 and 3. Selected bond distances and angles are listed in Table 2. Complex **4** is a tetrametallic Pt_2Pd_2 unit in which the four metal atoms are bridged by phosphide ligands. The atoms

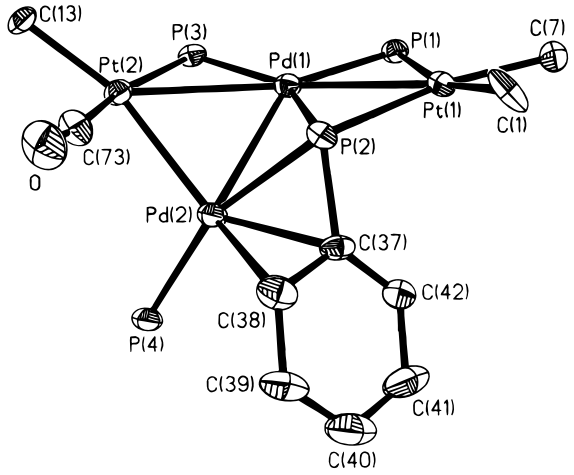

Figure 3. Schematic view of the central core of **4**.

Table 2. Selected Bond Lengths (Å) and Angles (deg) for $[Pt_2Pd_2(PPh_2)_3(C_6F_5)_3\{PPh_2(C_6F_5)\}(CO)]\cdot CHCl_3\cdot C_5H_{12}$ ($4\cdot CHCl_3\cdot C_5H_{12}$)

Pt(1)−C(7)	2.058(8)	Pd(1)−P(1)	2.220(2)
Pt(1)−P(2)	2.371(2)	Pd(1)−Pd(2)	2.7983(9)
Pt(2)−C(13)	2.065(8)	Pd(2)−C(37)	2.425(8)
Pt(2)−Pd(1)	2.8718(7)	Pt(1)−P(1)	2.305(2)
Pd(1)−P(2)	2.376(2)	Pt(2)−C(73)	1.922(9)
Pd(2)−P(2)	2.351(2)	Pt(2)−Pd(2)	2.7063(7)
Pt(1)−C(1)	2.100(9)	Pd(1)−P(3)	2.249(2)
Pt(1)−Pd(1)	2.7513(7)	Pd(2)−P(4)	2.342(2)
Pt(2)−P(3)	2.285(2)	Pd(2)−C(38)	2.649(8)
C(7)−Pt(1)−C(1)	84.1(3)	C(7)−Pt(1)−P(1)	86.8(2)
C(1)−Pt(1)−P(1)	166.5(2)	C(7)−Pt(1)−P(2)	166.6(2)
C(1)−Pt(1)−P(2)	84.3(2)	P(1)−Pt(1)−P(2)	105.68(7)
C(73)−Pt(2)−C(13)	94.4(4)	C(73)−Pt(2)−P(3)	164.9(3)
C(13)−Pt(2)−P(3)	97.4(2)	C(73)−Pt(2)−Pd(2)	69.3(3)
C(13)−Pt(2)−Pd(2)	161.3(2)	P(3)−Pt(2)−Pd(2)	100.28(5)
P(1)−Pd(1)−P(3)	107.61(8)	P(1)−Pd(1)−P(2)	108.31(8)
P(3)−Pd(1)−P(2)	143.73(8)	P(1)−Pd(1)−Pd(2)	142.81(6)
P(3)−Pd(1)−Pd(2)	98.49(6)	P(2)−Pd(1)−Pd(2)	53.29(5)
Pt(1)−Pd(1)−Pd(2)	101.71(2)	P(4)−Pd(2)−C(37)	118.0(2)
P(4)−Pd(2)−C(38)	101.9(2)	P(2)−Pd(2)−Pt(2)	97.38(6)
Pd(1)−P(1)−Pt(1)	74.86(7)	Pd(2)−P(2)−Pd(1)	72.60(6)
Pt(1)−P(2)−Pd(1)	70.85(6)	Pd(1)−P(3)−Pt(2)	78.60(7)
C(37)−P(2)−Pd(2)	69.8(2)	C(37)−P(2)−Pt(1)	110.3(3)
C(37)−P(2)−C(43)	107.7(4)	C(43)−P(2)−Pd(2)	111.0(3)
C(43)−P(2)−Pt(1)	114.5(3)	C(43)−P(2)−Pd(1)	119.6(3)

Pt(1), C(1), C(7), P(1), Pd(1), P(3), Pt(2), C(73), and O lie almost in a plane (see Figure 3), with a maximum deviation for the Pd(1) center (0.203 Å). P(2) is located below this plane, at 0.517 Å. Complex **4** can be regarded as the union of the "$Pd(2)(PPh_2C_6F_5)$" fragment to the planar moiety described above through metal−metal interactions and a $P(2)Ph_2$ bridging ligand. Pd(1), Pd(2), and Pt(2) form a nearly equilateral triangle. The internal angles are Pd(1)−Pt(2)−Pd(2) 60.13(2)°, Pt(2)−Pd(1)−Pd(2) 57.00(2)°, and Pt(2)−Pd(2)−Pd(1) 62.87(2)°, and the intermetallic distances are Pt(2)−Pd(1) 2.8718(7), Pd(1)−Pd(2) 2.7983(9), and Pt(2)−Pd(2) 2.7063(7) Å, all three within bonding distance.[13] Pd(2) is also bonded to P(2) with an interatomic distance of 2.351(2) Å. The geometry around atom P(2) is very unusual, since it is five-coordinate[12,14] and acts as a triple bridge between three of the metal atoms (Pt(1),

(13) (a) Berry, D. E.; Bushnell, G. W.; Dixon, K. R.; Moroney, P. M.; Wan, C. *Inorg. Chem.* **1985**, *24*, 2634. (b) Leoni, P.; Manetti, S.; Pasquali, M.; Albinati, A. *Inorg. Chem.* **1996**, *35*, 6045. (c) Bender, R.; Braunstein, P.; Dedieu, A.; Ellis, P. D.; Huggins, B.; Harvey, P. D.; Sappa, E.; Tiripicchio, A. *Inorg. Chem.* **1996**, *35*, 1223.

Pd(1), and Pd(2)) of the complex. The three P(2)−M distances are almost equal (2.371(2) Å for Pt(1), 2.376(2) Å for Pd(1), and 2.351(2) Å for Pd(2)) and longer than the other phosphide−metal distances present in **4** (see Table 2). Moreover, there are also relatively short distances between the Pd(2) center and two carbon atoms of one phenyl ring of the P(2) phosphide ligand, indicating a possible η^2-arene interaction. The complexes $[Ru_4(\mu\text{-H})(CO)_{10}(\mu\text{-}PPh_2)(\mu\text{-}PPh_2C_6H_4)]$[15] and $[NBu_4][Pt_3(\mu\text{-}PPh_2)_2(C_6F_5)_5]$[5a] show a similar unusual bridging phosphide in which there is an M−P distance that is longer than the other two, with the metal center M simultaneously bonded to one of the phenyl rings of the phosphide through an η^2-arene interaction. However, the Pd(2)−C distances in **4** are 2.425(8) Å for C(37) and 2.649(8) Å for C(38), longer than the ones found in the complexes mentioned above, indicating that in **4** the η^2-arene interaction is weaker. The coordination sphere of the Pd(2) center is completed by a $PPh_2C_6F_5$ ligand which, as we will see below, is also present in the starting material **3**, as revealed by its NMR spectra.

Pt(2) lies in the center of a square planar environment formed by the P(3)PPh_2 phosphide, one carbonyl, and one pentafluorophenyl ligand, the fourth coordination position being taken by the Pd(2) atom. This geometry forces the C(13) atom to be located 1.309 Å above the main molecular plane described above. Phosphide P(3) bridges the Pt(2) and Pd(1) centers. The angle Pt(2)−P(3)−Pd(1) is small (78.60(7)°), consistent with the short intermetallic distance.

The environment of the Pd(1) atom is very distorted. It is doubly bridged to Pt(1) by two phosphide ligands. The geometry of the Pd(1)$(\mu\text{-}PPh_2)_2$Pt(1) fragment, small Pd−P−Pt and large P−M−P angles, is commonly found[6] for systems in which short intermetallic distances are present. For **4**, the Pt(1)−Pd(1) distance is 2.7513(7) Å. Pt(1) is also bonded to two pentafluophenyl ligands, thus completing the square planar coordination sphere.

If the phenyl−platinum interaction observed in **4** represents a classical two electron bonding interaction, this structure gives a total valence electron count of 58, which would be in agreement with the presence of three metal−metal bonds. However, the crystal structure reveals the existence of four short metal−metal distances, in agreement with a total valence electon count of 56. The values of these distances are quite similar, with a difference of 0.17 Å between the longest and the shortest. As can be seen, complex **4** shows some remarkable features: (i) the four metal centers present mixed formal oxidation states, since they have to supply an overall charge of 6+, (ii) a PPh_2 group acts as a triply bridging ligand. Only rarely[12,14,15] do such ligands display μ^3-PR_2 coordination with three metal centers involved, and (iii) a new phosphine ligand, $PPh_2(C_6F_5)$, is coordinated to a palladium center.

In the IR spectrum of complex **4**, the X-sensitive modes of the C_6F_5 groups appear as two broad absorptions with different intensities. Besides the strong signals around 1500 and 950 cm^{-1}, two other absorptions of lower intensity are observed at higher frequencies (1515 and 977 cm^{-1}), the latter probably being due to the C_6F_5 group bonded to the P atom. An absorption at 2025 cm^{-1} is due to ν(C≡O). This value is lower than the ones found for the corresponding ν(C≡O) in complex **2**, indicating a larger degree of π-back donation in the Pt−CO bond. The ^{19}F NMR spectrum of **4** shows, in the usual region of *o*-F atoms, five signals with platinum satellites and an intensity ratio of 2:1:1:1:1. The most intense signal is assigned to *o*-F of the C_6F_5 group *cis* to the CO group and the other ones to the four inequivalent *o*-F atoms of the two C_6F_5 groups mutually *cis*. Signals due to the *m*-F and *p*-F atoms of these C_6F_5 groups appear, as expected, from −160 to −165 ppm, but an unambiguous assignment for all these *m*-F and *p*-F cannot be carried out. Moreover, the spectrum shows signals due to another type of C_6F_5 group. The ones due to *o*-F (−127.1 ppm, no platinum satellites) and *p*-F (−150.2 ppm) appear in a striking region, while the signal due to *m*-F is in the same region as the *m*-F and *p*-F signals of the other C_6F_5 groups. These signals can be assigned to the phosphine pentafluorophenyl ring. Similar chemical shifts have been observed in other pentafluorophenyl organic ligands.[16]

The ^{31}P NMR spectrum of **4** shows four signals. Three of them, with platinum satellites, appear from 270 to 150 ppm and are assigned to P atoms of the PPh_2 groups. These downfield chemical shifts are consistent with short metal−metal distances and small M−P−M angles in the "M$(\mu\text{-}PPh_2)_x$M" ($x = 1$ or 2) systems. The signal due to the P atom of the $PPh_2C_6F_5$ phosphine ligand appears at 23.9 ppm and has no platinum satellites.

Structural Characterization of 3. All our attemps to grow crystals of **3** suitable for an X-ray study have proven unsuccessful. So, the structure of complex **3** can only be established on the basis of spectroscopic data and by comparing it with the structure of **4**.

The IR spectrum of complex **3** shows two broad absorptions of different intensities which can be assigned to the X-sensitive mode of the C_6F_5 groups. As in complex **4**, beside the strong signals around 1500 and 950 cm^{-1}, two other absorptions of lower intensity are observed at higher frequencies (1516 and 978 cm^{-1}), indicating that, as in **4**, the $PPh_2C_6F_5$ ligand is present in complex **3**.

The ^{19}F NMR spectrum of **3** shows three signals with platinum satellites and an intensity ratio of 2:2:2 due to the *o*-F atoms of the three C_6F_5 groups bonded to the platinum centers. Signals due to the *m*-F and *p*-F atoms of these C_6F_5 groups appear overlapped in the range from −160 to −165 ppm. Moreover, there are two signals with an intensity ratio of 2:1 at *ca.* −130 and −150 ppm. The chemical shifts of these signals indicate that complex **3**, as with complex **4**, must contain a $PPh_2C_6F_5$ ligand.

The ^{31}P NMR spectrum of **3** shows four signals in the same region as that for complex **4**. Unlike complex **4**, all of these signals show platinum satellites. This indicates that in complex **3** the $PPh_2C_6F_5$ ligand has to be bonded to a Pt center.

A reasonable structure for complex **3**, which agrees with all of these spectroscopic data, is schematized in

(14) (a) Gol, F.; Knuppel, P. C.; Stelzer, O.; Sheldrick, W. S. *Angew. Chem., Int. Ed. Engl.* **1988**, *27*, 956. (b) Brauer, D. J.; Knuppel, P. C.; Stelzer, O. *J. Chem. Soc., Chem. Commun.* **1988**, 551. (c) Jones, R. A.; Stuart, A. L.; Wright, T. C. *J. Am. Chem. Soc.* **1983**, *105*, 7459.

(15) Corrigan, J. F.; Doherty, S.; Taylor, N. J.; Carty, A. J. *J. Am. Chem. Soc.* **1992**, *114*, 7557.

(16) (a) Usón, R.; Forniés, J.; Espinet, P.; Lalinde, E.; Jones, P. G.; Sheldrick, G. M. *J. Chem. Soc., Dalton Trans.* **1982**, 2389. (b) Usón, R.; Forniés, J.; Espinet, P.; Lalinde, E. *J. Organomet. Chem.* **1983**, *254*, 371.

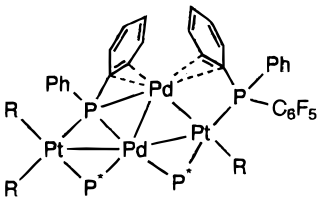

Figure 4. Schematic representation of the structure proposed for $[Pt_2Pd_2(\mu\text{-}PPh_2)_3(C_6F_5)_3(PPh_2C_6F_5)]$ (**3**).

Figure 4, in which probably one of the palladium centers has to display two η^2-C_6H_5−Pd weak interactions. The formation of complex **3** is most unusual since it requires a reductive coupling between a phosphido ligand and a pentafluorophenyl group to afford a tertiary phosphine, which is a very rare process. In fact, it is well-known that tertiary phosphine ligands can be converted thermally to phosphido bridging species through the breaking of a P−C bond and formation of new M−P and M−C bonds.[13c,17] Examples of reductive coupling between a phosphido group and a one-electron donor ligand to afford a tertiary phosphine are rather scarce.[18] Braunstein *et al*. have recently reported[19] the first cluster-mediated conversion of $M-C_6H_5$ into a $P-C_6H_5$ bond, a coupling reaction between a PPh_2 bridge and a phenyl group to give a PPh_3 ligand. Since it is well-known that the $M-C_6F_5$ bonds are more stable than the corresponding $M-C_6H_5$ bonds,[20] the formation of complex **3** throught a reductive coupling is most unusual.

Finally, it is also noteworthy that the reaction of **3** with CO, which should result in the breaking of the weak η^2-C_6H_5−Pd interactions, does simultaneously produce a migration of the phosphine ligand to the palladium center. The ability of CO to act as a bridging ligand[21] and the higher stability of the Pt−CO bond as compared to Pd−CO could be the reason for this phosphine migration. In addition, it is also noteworthy that although the reaction is carried out in an excess of CO, only one of the proposed η^2-C_6H_5−Pd interactions is broken.

Experimental Section

General Comments. C, H, and N analyses were performed with a Perkin-Elmer 240B microanalyzer. IR spectra were recorded on a Perkin-Elmer 599 spectrophotometer (Nujol mulls between polyethylene plates in the range 4000−200 cm^{-1}). NMR spectra were recorded on a Varian Unity 300 instrument with $CFCl_3$ and 85% H_3PO_4 as external references for ^{19}F and ^{31}P, respectively. Conductivities (acetone, $c \approx 5 \times 10^{-4}$ M) were measured with a Philips PW 9509 conductimeter. Mass spectra were recorded on a VG-Autospec spectrometer operating at 30 kV, using the standard Cs-ion FAB gun and 3-nitrobenzyl alcohol (3-NOBA) as the matrix. Literature methods were used to prepare the starting complexes $[NBu_4]_2[\{(C_6F_5)_2Pt(\mu\text{-}PPh_2)_2M(\mu\text{-}Cl)\}_2]$.[2a]

Preparation of $[NBu_4][(C_6F_5)_2Pt(\mu\text{-}PPh_2)_2PtCl(CO)]$ (1). CO was bubbled into a CH_2Cl_2 (10 mL) solution of $[NBu_4]_2[\{(C_6F_5)_2Pt(\mu\text{-}PPh_2)_2Pt(\mu\text{-}Cl)\}_2]$ (400 mg, 0.146 mmol) at room temperature for 20 min. The resulting solution was treated with 20 mL of *n*-hexane, and CO was bubbled for 15 min so that an oily residue was obtained. The stirring of this oily residue for 2 h resulted in the precipitation of a white solid, which was filtered off and washed with *n*-hexane (362 mg, 89% yield). Anal. Calcd for $C_{53}ClF_{10}H_{56}NOP_2Pt_2$: C, 45.45; H, 4.0; N, 1.0. Found: C, 45.75; H, 4.05; N, 1.0. $\Lambda_M = 102\ \Omega^{-1}\ cm^2\ mol^{-1}$. IR (Nujol): 783, 776 cm^{-1} (X-sensitive, C_6F_5); 2075 cm^{-1} (ν(C≡O)). FAB-MS: *m*/*z* 1130 ($[M - CO]^-$). ^{19}F NMR (20 °C, acetone-d_6, 282.4 MHz) δ: −116.1(4 *o*-F, $^3J_{Pt-F} = 325.2$ Hz), −167.2 to −168.6 (6 *m*-F + *p*-F). $^{31}P\{^1H\}$ NMR (20 °C, acetone-d_6, 121.4 MHz) δ: −137.1 ($^1J_{Pt-P} = 1941.6$ Hz, $^2J_{P-P} = 147.4$ Hz), −142.9 ($^1J_{Pt-P} = 1958.7$, 1821.7 Hz).

Preparation of $[Pt_4(\mu\text{-}PPh_2)_4(C_6F_5)_4(CO)_2]$ (2). To a stirred solution of **1** (200 mg, 0.143 mmol) in CH_2Cl_2 (15 mL), $AgClO_4$ was added (31 mg, 0.149 mmol). After 3 h of stirring, the mixture was filtered off and the solvent was removed under vacuum. *i*-PrOH (8 mL) was added, and by stirring, an orange solid **2** crystallized, which was filtered off and washed with 1 mL of *i*-PrOH (104 mg, 65%). Anal. Calcd for $C_{74}F_{20}H_{40}O_2P_4Pt_4$: C, 39.6; H, 1.8. Found: C, 39.4; H, 1.8. IR (Nujol): 796, 782 cm^{-1} (X-sensitive, C_6F_5); 2082, 2056 cm^{-1} (ν(C≡O)). FAB-MS: *m*/*z* 2189 ($[M - 2CO]^+$). ^{19}F NMR (20 °C, $CDCl_3$, 282.4 MHz) δ: −117.1 (2 *o*-F, $^3J_{Pt-F} = 366.2$ Hz), −118.0 (2 *o*-F, $^3J_{Pt-F} = 304.2$ Hz), −119.2 (4 *o*-F, $^3J_{Pt-F} = 300.7$ Hz), −159.4 (2 *m*-F), −160.2 (1 *p*-F), −161.2 (1 *p*-F), −163.0 (4 *m*-F), −163.4 (2 *m*-F), −164.1 (2 *p*-F). $^{31}P\{^1H\}$ NMR (20 °C, $CDCl_3$, 121.4 MHz) δ: 275.7 (ddd, P(4), $^1J_{Pt(4)-P(4)} = 1097.8$ Hz, $^1J_{Pt(3)-P(4)} = 1914.2$ Hz, $^2J_{P(4)-P(2)} = 119.6$ Hz, $^2J_{P(4)-P(3)} = 64.3$ Hz, $^3J_{P(4)-P(1)} = 28.9$ Hz), 257.2 (pseudo t, br, P(3), $^1J_{Pt(4)-P(3)} = 1312.7$ Hz, $^1J_{Pt(3)-P(3)} = 2104.4$ Hz), 147.1 (dd, P(2), $^1J_{Pt-P(2)} = 2875.4$, 2792.7 Hz, $^2J_{Pt(4)-P(2)} = 81.5$ Hz, $^2J_{P(4)-P(2)} = 119.6$ Hz, $^2J_{P(3)\text{ or }P(1)-P(2)} = 7.3$ Hz), −6.9 (s very br, P(1), $^1J_{Pt-P(1)} = 2652.3$, 1741.2 Hz, $^2J_{Pt(3)-P(1)} = 237.9$ Hz).

Preparation of $[Pt_2Pd_2(\mu\text{-}PPh_2)_3(C_6F_5)_3(PPh_2C_6F_5)]$ (3). To a CH_2Cl_2 solution (15 mL) of $[NBu_4]_2[\{(C_6F_5)_2Pt(\mu\text{-}PPh_2)_2Pd(\mu\text{-}Cl)\}_2]$ (500 mg, 0.195 mmol) was added $AgClO_4$ (95 mg, 0.458 mmol). After 3 h of stirring, the mixture was filtered off and the solution was evaporated almost to dryness. The addition of *i*-PrOH (10 mL) caused the precipitation of a purple solid **3**, which was filtered off and washed with small portions (2 × 1 mL) of *i*-PrOH (314 mg, 80%). Anal. Calcd for $C_{72}F_{20}H_{40}P_4Pd_2Pt_2$: C, 43.0; H, 2.0. Found: C, 43.1; H, 1.8. IR (Nujol): 1516, 978 cm^{-1} (C_6F_5); 791, 780 cm^{-1} (X-sensitive, C_6F_5). FAB-MS: *m*/*z* 2012 ($[M]^+$). ^{19}F NMR (20 °C, $CDCl_3$, 282.4 MHz) δ: −115.9 (2 *o*-F, $^3J_{Pt-F} = 307.8$ Hz), −118.3 (2 *o*-F, $^3J_{Pt-F} = 395.1$ Hz), −118.6 (2 *o*-F, $^3J_{Pt-F} = 336.9$ Hz), −130.4 (2 *o*-F, $PPh_2C_6F_5$), −150.0 (1 *p*-F, $PPh_2C_6F_5$), −162.4 (2 *m*-F, $PPh_2C_6F_5$), −161.4 and −164.0 (9 *m*-F + *p*-F). $^{31}P\{^1H\}$ NMR (20 °C, $CDCl_3$, 121.4 MHz) δ: 261.8 (s, br, $^1J_{Pt-P} = 1595.5$ Hz), 190.6 (d, br, $^1J_{Pt-P} = 1227.5$ Hz, $J_{P-P} = 70.9$ Hz), 139.6 (dm, br, $^1J_{Pt-P} = 2553.7$ Hz, $J_{P-P} \approx 360$ Hz), 5.7 (d, $PPh_2C_6F_5$, $^1J_{Pt-P} = 2843.6$ Hz, $J_{P-P} = 363.8$ Hz).

Preparation of $[Pt_2Pd_2(\mu\text{-}PPh_2)_3(C_6F_5)_3(PPh_2C_6F_5)(CO)]$ (4). CO was bubbled through a CH_2Cl_2 (8 mL) solution of **3** (100 mg, 0.050 mmol) at room temperature for 20 min. *n*-Hexane (20 mL) was added to the resulting solution, and then CO was bubbled through the solution for 20 min. After filtration, the solution was left to stand in the freezer (−18 °C) for 1 week. The resulting purple solid was filtered off and washed with 2 × 1 mL of cold *n*-hexane (**4**, 50 mg, 49%). Anal. Calcd for $C_{73}F_{20}H_{40}OP_4Pd_2Pt_2$: C, 43.0; H, 2.0. Found: C, 42.8; H, 1.8. IR (Nujol): 1515, 977 cm^{-1} (C_6F_5); 790, 779 cm^{-1} (X-

(17) (a) Dubois, R. A.; Garrou, P. E. *Organometallics* **1986**, *5*, 460. (b) Shiu, K.-B.; Jean, S.-W.; Wang, H.-J.; Wang, S.-L.; Liao, F.-L.; Wang, J.-C.; Liou, L.-S. *Organometallics* **1997**, *16*, 114.(c) García, G.; García, M. E.; Melón, S.; Riera, V.; Ruiz, M. A.; Villafañe, F. *Organometallics* **1997**, *16*, 624.

(18) (a) Shulman, P. M.; Burkhardt, E. D.; Lundquist, E. G.; Pilato, R. S.; Geoffroy, G. L.; Rheingold, A. L. *Organometallics* **1987**, *6*, 101. (b) Blum, O.; Frolow, F.; Milstein, D. *J. Chem. Soc., Chem. Commun.* **1991**, 258. (c) Kong, K. C.; Chen, C. H. *J. Am. Chem. Soc.* **1991**, *113*, 6313.

(19) Archambault, C.; Bender, R.; Braunstein, P.; De Cian, A.; Fischer, J. *J. Chem. Soc., Chem. Commun.* **1996**, 2729.

(20) Usón, R.; Forniés, J.; Tomás, M. *J. Organomet. Chem.* **1988**, *358*, 525.

(21) Oudet, P.; Moïse, C; Kubicki, M. M. *Inorg. Chim. Acta* **1996**, *247*, 263.

Table 3. Crystal Data and Structure Refinement

complex	**2**·$2CH_2Cl_2$	**4**·$CHCl_3.C_5H_{12}$
empirical formula	$C_{74}H_{40}F_{20}O_2P_4Pt_4$·$2CH_2Cl_2$	$C_{73}H_{40}F_{20}OP_4Pd_2Pt_2$·$CHCl_3$·$C_5H_{12}$
unit cell dimens		
a (Å)	17.9838(14)	15.227(2)
b (Å)	23.281(2)	15.2923(12)
c (Å)	19.7896(15)	17.229(2)
α (deg)	90	87.625(8)
β (deg)	97.146(14)	84.326(9)
γ (deg)	90	85.793(7)
volume (Å^3), *Z*	8221.1(11), 4	3979.1(7), 2
wavelength (Å)	0.71073	
temperature (K)	150(1)	150(1)
radiation	graphite monochromated Mo Kα	
cryst syst	monoclinic	triclinic
space group	$P2_1/n$	$P\bar{1}$
cryst dimens (mm)	0.70 × 0.50 × 0.30	0.50 × 0.40 × 0.20
abs coeff (mm^{-1})	7.082	4.222
transmission factors	1.000, 0.255	0.989, 0.603
abs corr	*ψ* scans	*ψ* scans
diffractometer	Enraf-Nonius CAD4	Siemens P4
2*θ* range for data collection (deg)	4.0−50.0 (+*h*, +*k*, ±*l*)	4.0−50.0 (+*h*, ±*k*, ±*l*)
no. of reflns collected	14 906	14 549
no. of independent reflns	14 409 [*R*(int) = 0.0309]	13 975 [*R*(int) = 0.0465]
refinement method	full-matrix least-squares on F^2	
goodness-of-fit on F^2	1.068	1.023
final *R* indices [$I > 2\sigma(I)$][a]	R1 = 0.0422	R1 = 0.0435
	wR2 = 0.1066	wR2 = 0.0866
R indices (all data)	R1 = 0.0601	R1 = 0.0781
	wR2 = 0.1193	wR2 = 0.1043

[a] $wR2 = [\sum w(F_o^2 - F_c^2)^2/\sum wF_o^4]^{0.5}$; $R1 = \sum||F_o| - |F_c||/\sum|F_o|$.

sensitive, C_6F_5). FAB-MS: *m*/*z* 2012 ([M − CO]$^+$). ^{19}F NMR (20 °C, $CDCl_3$, 282.4 MHz) *δ*: −114.0 (2 *o*-F, $^3J_{Pt-F}$ = 382.0 Hz), −116.3 (1 *o*-F, $^3J_{Pt-F}$ = 290.1 Hz), −118.0 (1 *o*-F, $^3J_{Pt-F}$ = 355.0 Hz), −119.1 (1 *o*-F, $^3J_{Pt-F}$ = 280.2 Hz), −119.7 (1 *o*-F, $^3J_{Pt-F}$ = 295.5 Hz), −127.1 (2 *o*-F, $PPh_2C_6F_5$), −150.2 (1 *p*-F, $PPh_2C_6F_5$), −160.3 (2 *m*-F), −161.0 (2 *m*-F), −161.5 (1 *p*-F), −163.2 to −164.6 (6 *m*-F + *p*-F). ^{31}P{^{1}H} NMR (20 °C, $CDCl_3$, 121.4 MHz) *δ*: 266.9 (s, very br, P(1), $^1J_{Pt(1)-P(1)}$ = 1567.1 Hz), 174.4 (ddd br, P(2), $^1J_{Pt(1)-P(2)}$ = 1239.9 Hz, $^2J_{P(2)-P(4)}$ = 140.2 Hz, $^2J_{P(2)-P(3)}$ = 92.1 Hz, $^2J_{P(2)-P(1)}$ = 17.8 Hz), 152.7 (dd, P(3), $^1J_{Pt(2)-P(3)}$ = 2566.5 Hz, $^2J_{Pt(1)-P(3)}$ = 59.1 Hz, $^2J_{P(2)-P(3)}$ = 92.1 Hz, $^2J_{P(1)-P(3)}$ = 35.0 Hz), 23.9 (dd, P(4), $^2J_{P(2)-P(4)}$ = 140.2 Hz, $^3J_{P(4)-P(1)}$ = 15.1 Hz).

Preparation of Crystals of 2 and 4 for X-ray Structure Determinations. Suitable crystals of **2** were obtained by slow diffusion of *n*-hexane into a solution of 0.025 g of the complex in CH_2Cl_2. Suitable crystals of **4** were obtained by slow diffusion of *n*-pentane into a solution of 0.025 g of the complex in $CHCl_3$.

Crystal Structure Analysis of $[Pt_4(C_6F_5)_4(PPh_2)_4(CO)_2]$·$2CH_2Cl_2$ (2·$2CH_2Cl_2$). Crystal data and other details of the structure analysis are presented in Table 3. A crystal of **2** was mounted at the end of a quartz fiber and held in place with a fluorinated oil. Unit cell dimensions were determined from 25 centered reflections in the range 22.8° < 2 *θ* < 31.7°. Three check reflections remeasured after every 2 h showed no decay of the crystal over the period of data collection. An absorption correction was applied based on 555 azimuthal scan data. The structure was solved by Patterson and Fourier methods. All calculations were carried out using the program SHELXL-93.[22] All non-hydrogen atoms were assigned anisotropic displacement parameters and refined without positional constraints. The hydrogen atoms of the complex were constrained to idealized geometries and assigned isotropic displacement parameters of $1.2U_{iso}$ of their attached atom. Four molecules of the dichloromethane solvent were found (confirmed by ^{1}H NMR spectroscopy), of which one (C(76), Cl(3), and Cl(4)) was assigned 0.5 occupancy and two (C(77), Cl(5), and Cl(6); C(78), Cl(7), and Cl(8)) 0.25 occupancy. For the latter two, interatomic bond distances and angles were constrained to idealized geometries. Full-matrix least-squares refinement of this model against F^2 converged to the final residual indices given in Table 3. Weights, *w*, were set equal to $[\sigma_c^2(F_o^2) + (aP)^2 + bP]^{-1}$, where $P = [0.333 \max\{F_o^2,0\} + 0.667F_c^2]$, $\sigma_c^2(F_o^2)$ is the variance in F_o^2 due to counting statistics, and $a = 0.0559$ and $b = 81.559$ were chosen to minimize the variation in *S* as a function of $|F_o|$. Final difference electron density maps showed 37 peaks above 1 e Å^{-3} (max 2.64; largest difference hole −1.88), all of them lying within 1.12 Å of the platinum atoms. Most of these peaks (31) have an electron density lower than 1.88 e Å^{-3}, and their presence can be explained on the basis of residual uncorrected absorption (the absorption coefficient is 7.082 mm^{-1}).

Crystal Structure Analysis of $[Pt_2Pd_2(PPh_2)_3(C_6F_5)_3\{PPh_2(C_6F_5)\}(CO)]$·$CHCl_3$·$C_5H_{12}$ (4·$CHCl_3$·C_5H_{12}). Crystal data and other details of the structure analysis are presented in Table 3. A crystal of **4** was mounted at the end of a glass fiber and held in place with a fluorinated oil. Unit cell dimensions were determined from 37 centered reflections in the range 20° < 2 *θ* < 30°. Three check reflections remeasured after every 297 ordinary reflections showed no decay of the crystal over the period of data collection. An absorption correction was applied based on 242 azimuthal scan data. The structure was solved by Patterson and Fourier methods. All calculations were carried out using the program SHELXL-93.[22] All non-hydrogen atoms were assigned anisotropic displacement parameters and refined without positional constraints, except for the solvent atoms. The hydrogen atoms of the complex were constrained to idealized geometries and assigned isotropic displacement parameters of $1.2U_{iso}$ of their attached carbon ($1.5U_{iso}$ for the methyl hydrogen atoms). Whereas the positions and thermal parameters of the atoms of the metal complex were found and refined without difficulty, the electron density corresponding to the solvent molecules was very diffuse. The model that gives the best results consists of one molecule of *n*-pentane disordered over two positions with 0.5 occupancy each and one molecule of $CHCl_3$ disordered over three positions with 0.333 occupancy each. Both solvents had been used in the obtention of the crystals, and signals of both were observed in the ^{1}H NMR spectrum of the crystals. The interatomic distances and angles in the solvent molecules were

(22) Sheldrick, G. M. *SHELXL-93, a program for crystal structure determination*; University of Göttingen, Göttingen, Germany, 1993.

constrained to idealized geometries, and the anisotropic thermal parameter of the carbon and chlorine atoms of each molecule were constrained to be the same. No attempts to include the solvent hydrogen atoms were made. Full-matrix least-squares refinement of this model against F^2 converged to the final residual indices given in Table 3. Weights, w, were set equal to $[\sigma_c^2(F_o^2) + (aP)^2 + bP]^{-1}$, where $P = [0.333 \max\{F_o^2,0\} + 0.667F_c^2]$, $\sigma_c^2(F_o^2)$ is the variance in F_o^2 due to counting statistics, and $a = 0.0369$ and $b = 14.87$ were chosen to minimize the variation in S as a function of $|F_o|$. Final difference electron density maps showed six peaks above 1 e Å^{-3} (1.26−1.05 e Å^{-3}; largest difference hole −1.06), all of them located in the solvent area.

Acknowledgment. We thank the Dirección General de Enseñanza Superior (Spain) for financial support (Project Nos. PB95-0003-CO2-01 and PB95-0792).

Supporting Information Available: Tables of full atomic positional and equivalent isotropic displacement parameters, anisotropic displacement parameters, full bond distances and bond angles, and hydrogen coordinates and isotropic displacement parameters for the crystal structures of complexes **2** and **4** (29 pages). Ordering information is given on any current masthead page.

OM9706469